

Елена Суровяткина

Нелинейная динамика

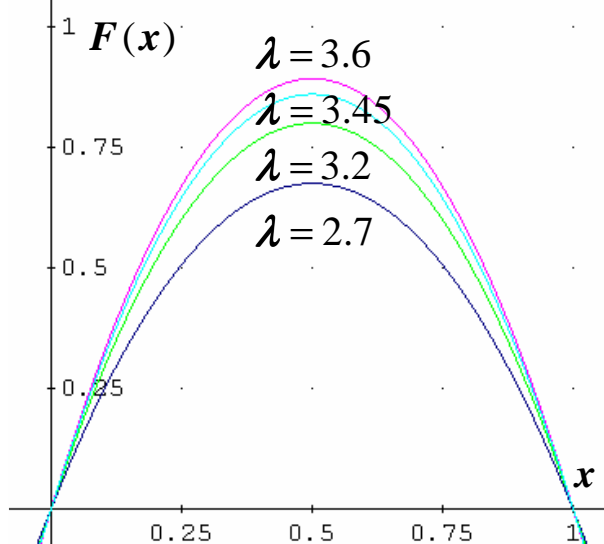
электрических процессов в
сердечной клетке человека.

*Физические и медицинские
аспекты*

Институт космических исследований Российской академии наук

LOGISTIC MAP

$$x_{n+1} = \lambda x_n (1 - x_n)$$



limit-cycle

2-cycle

4-cycle

CHAOS

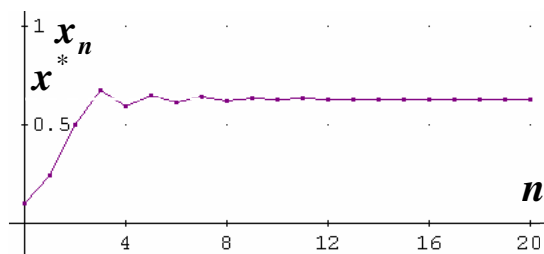
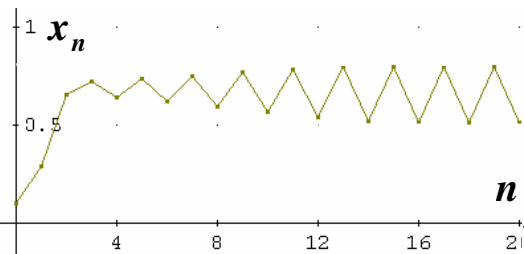
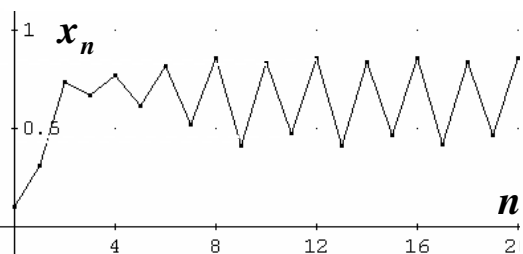


диаграмма Ламерея

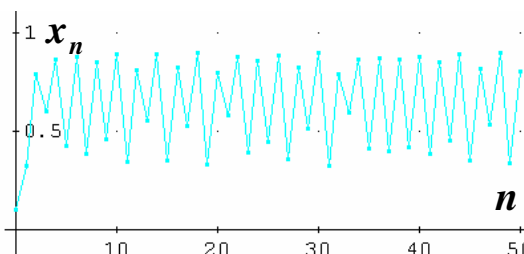
$\lambda = 2.8$



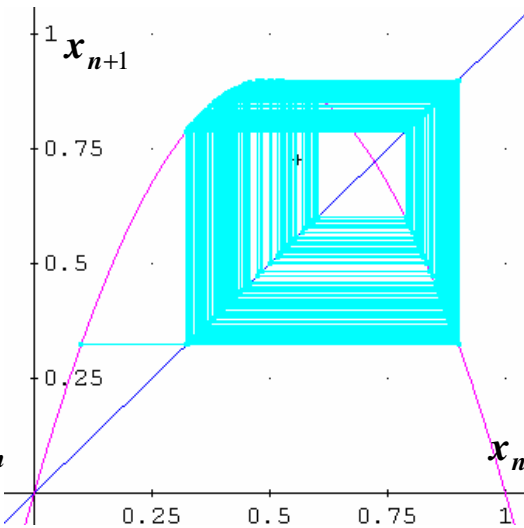
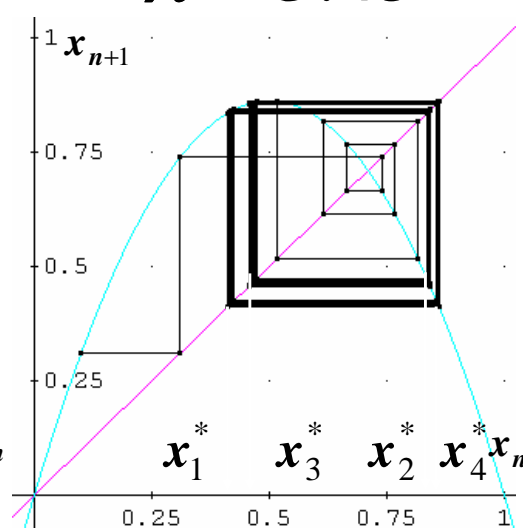
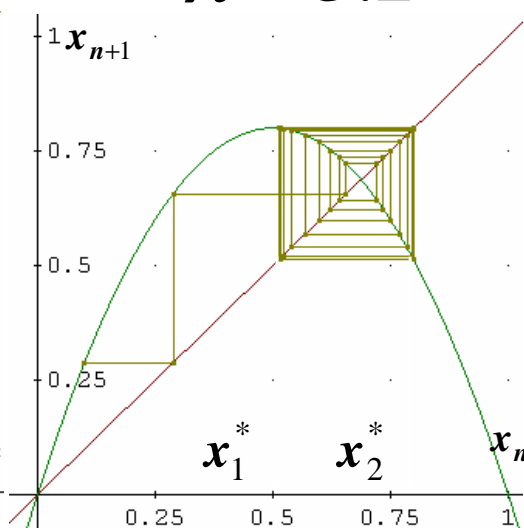
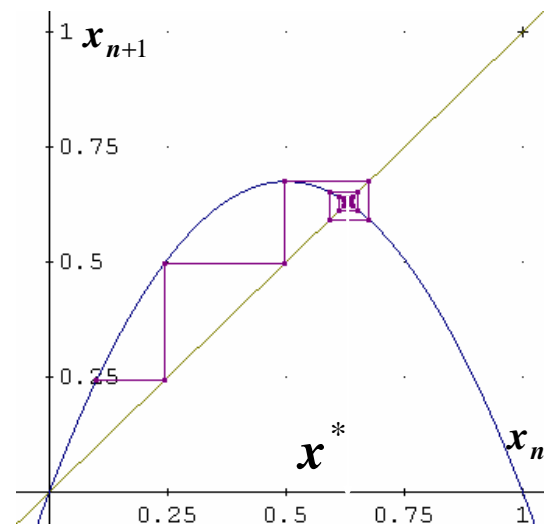
$\lambda = 3.2$



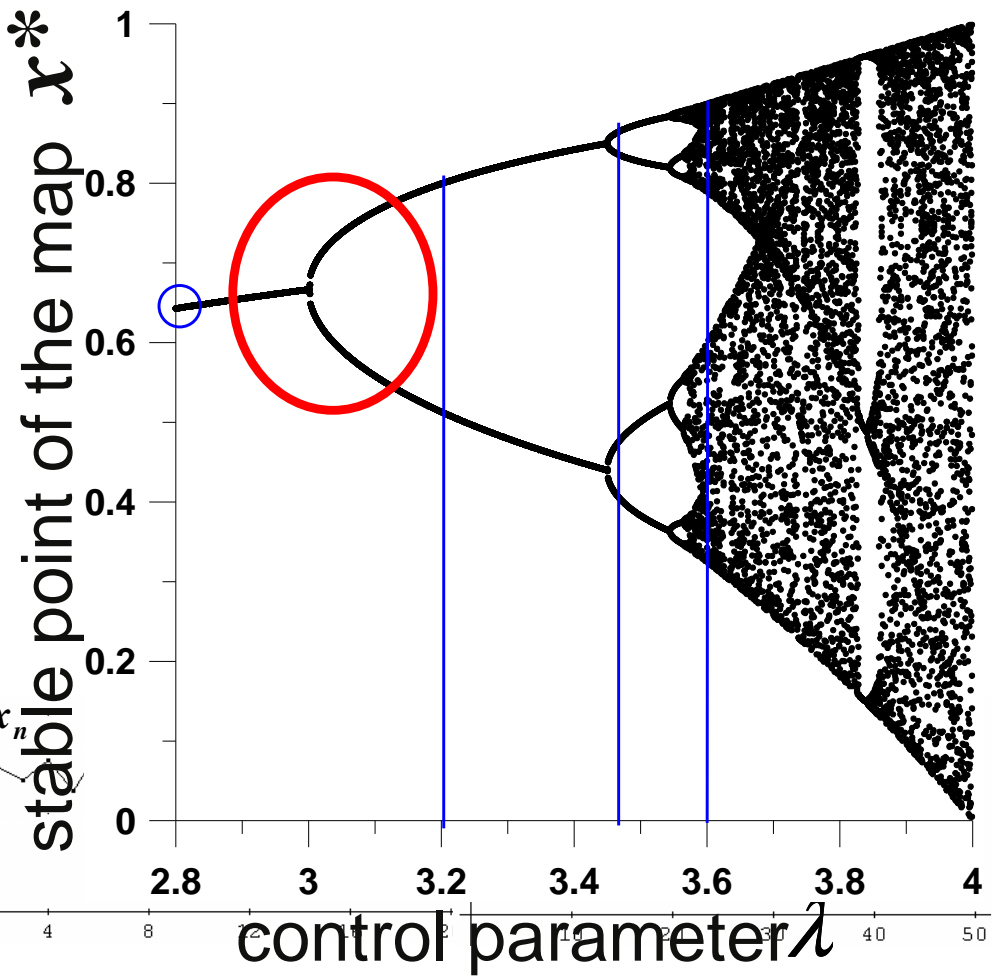
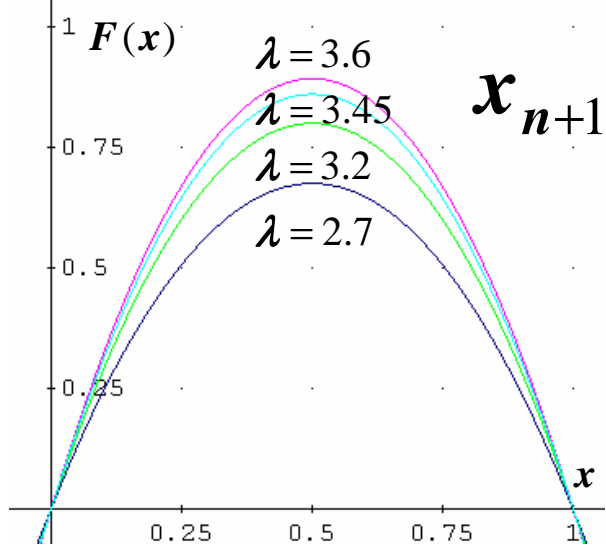
$\lambda = 3.45$



$\lambda = 3.6$



$$x_{n+1} = \lambda x_n (1 - x_n)$$



limit-cycle

2-cycle

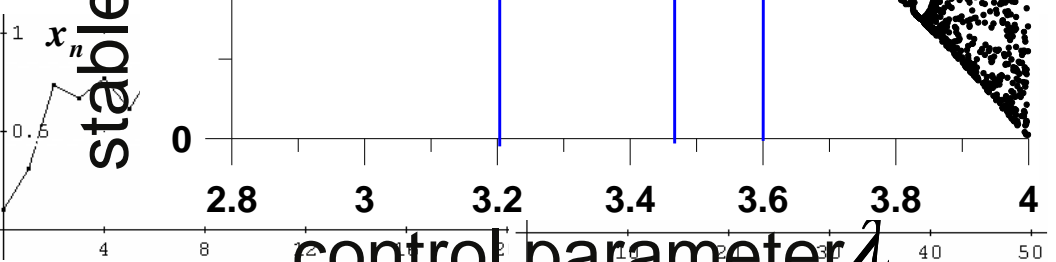
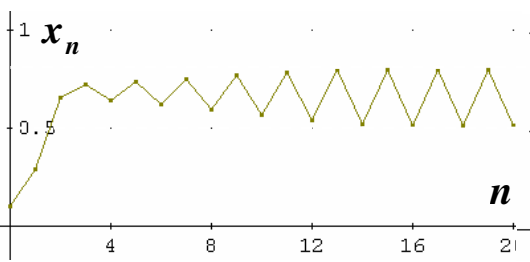
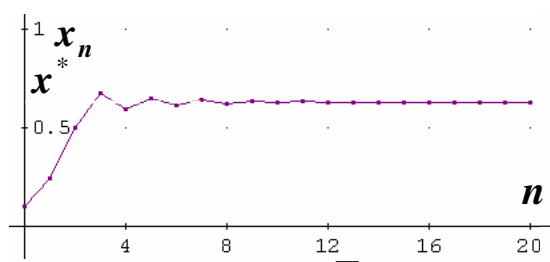
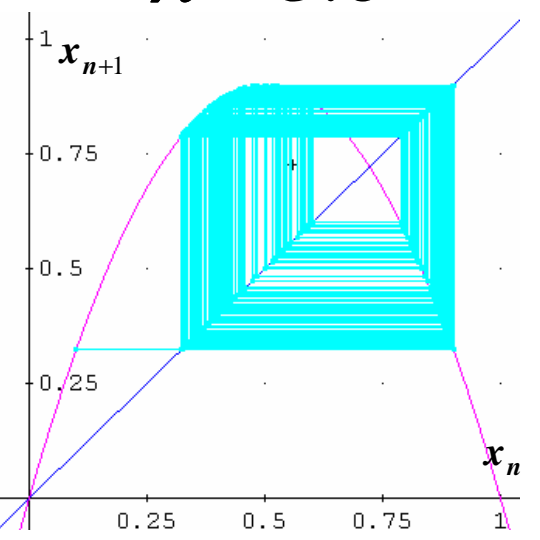
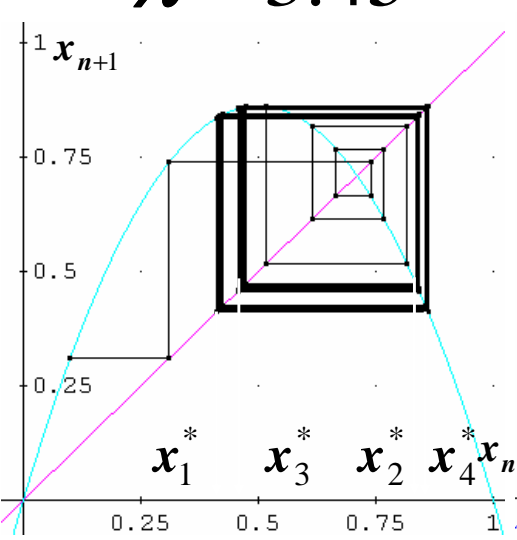
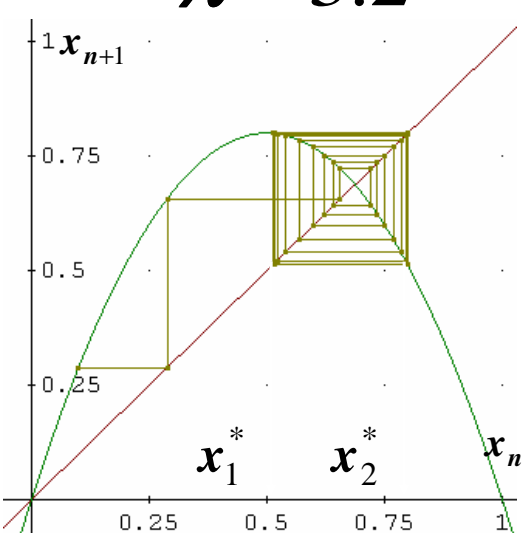
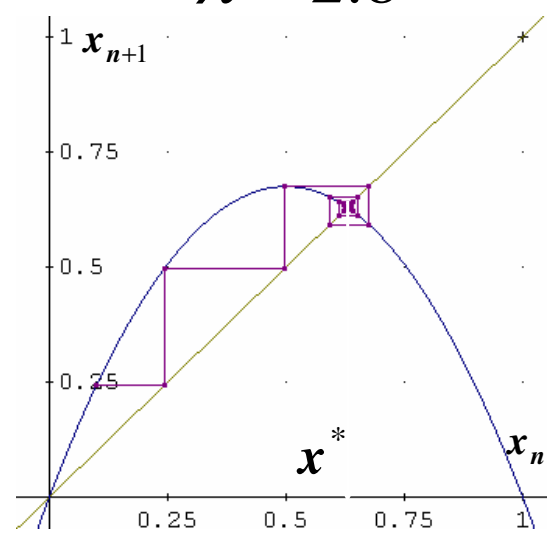


диаграмма Ламерея
 $\lambda = 2.8$

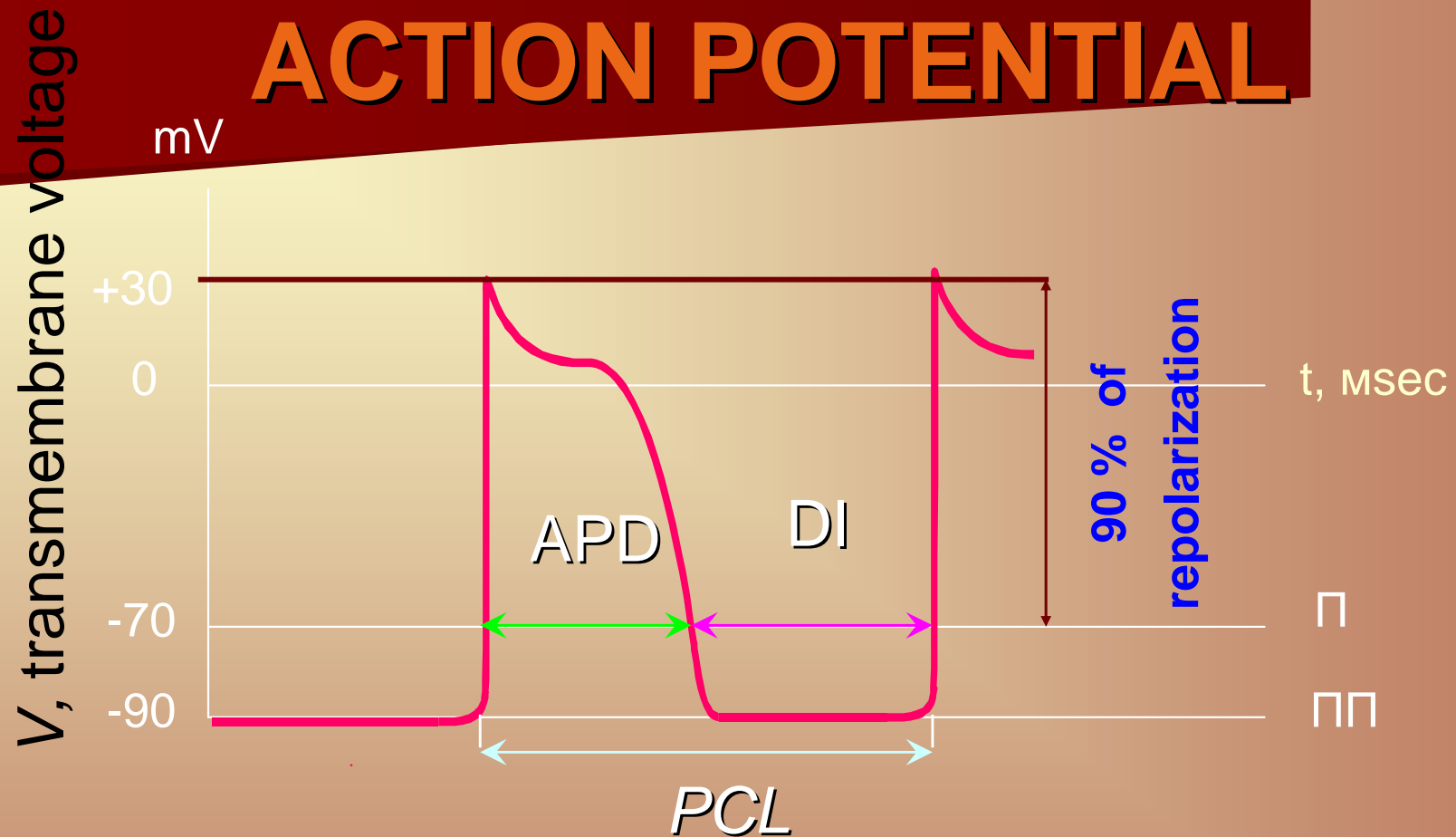
$\lambda = 3.2$

$\lambda = 3.45$

$\lambda = 3.6$



ACTION POTENTIAL



APD - action potential duration

DI - diastolic interval

PCL - pacing cycle length

From Pulsus to Pulseless

The Saga of Cardiac Alternans

James N. Weiss, Alain Karma, Yohannes Shiferaw, Peng-Sheng Chen, Alan Garfinkel, Zhilin Qu

$$APD_{n+1} = F(PCL - APD_n) = F(DI_n)$$

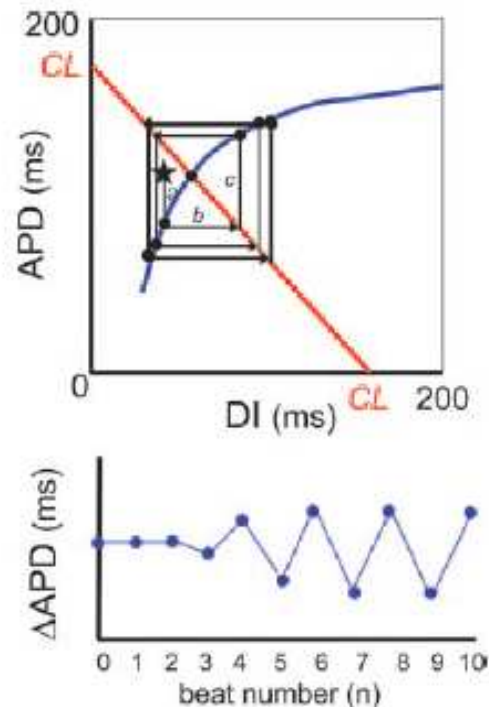
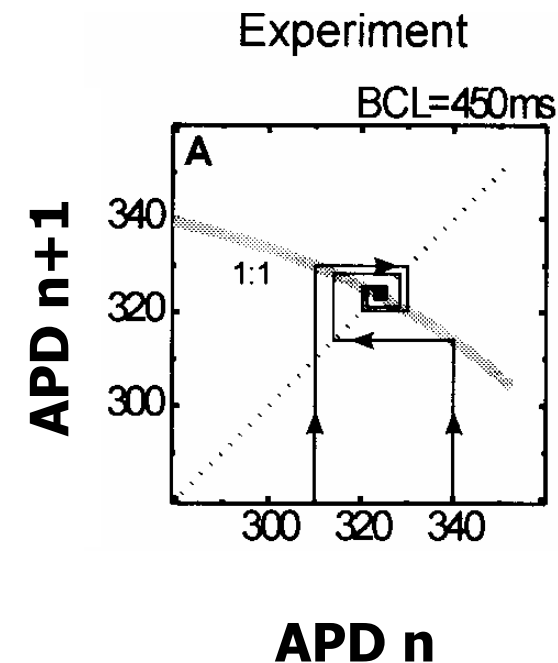


Figure 3. Cobweb diagram of APD alternans arising from steep APD restitution slope, after Nolasco and Dahlen.¹⁶ Blue line shows the APD restitution curve, and red line shows the $CL = APD + DI$ line. The top graph illustrates the effects of a perturbation, which shortens DI (asterisk), displacing the system from its unstable equilibrium point (solid black circle at the intersection of the two lines), resulting in persistent APD alternans, as shown in the bottom trace. See text for details.

$$APD_{n+1} = F(APD_n)$$



Yehia et al.

Chaos, Vol. 9, No. 4, 1999

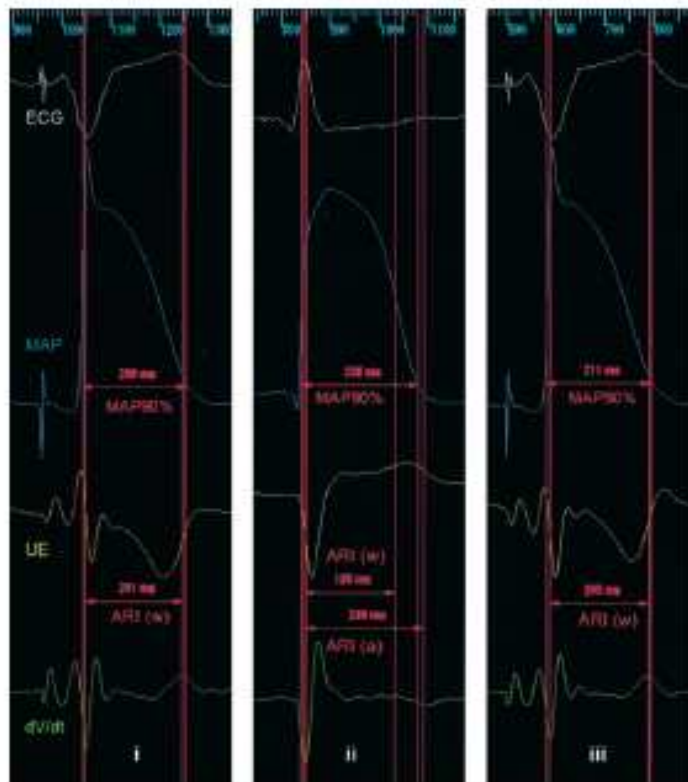
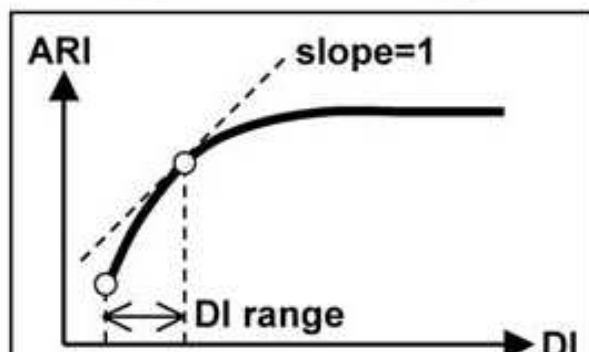


Figure 2. MAP recording, reconstructed UE, and first derivative (dV/dt) taken from same endocardial sites. ARI was measured by Wyatt between MAP90% duration and ARI for negative T wave (i), positive T pars.



Figure 3. Construction of restitution curve. Surface ECG shows drive train (S₁) and extrastimulus (S₂). MAP recording, reconstructed UE, and first derivative (dV/dt) were measured from same endocardial site and displayed simultaneously. ARI of S₂ was measured by alternative method.



Yue et al.
Noncontact Mapping of Electrical Restitution

JACC Vol. 46, No. 6, 2005
September 20, 2005:1067-75

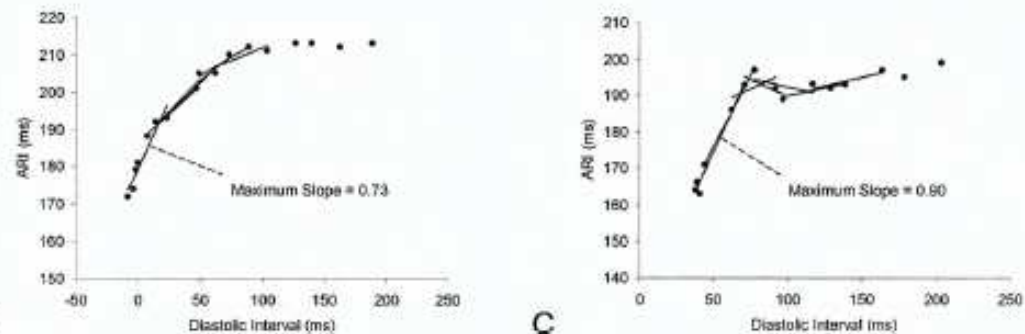


Figure 2. Activation-recovery interval (ARI) restitution and slope measurement. (A) Simultaneous measurement of ARIs at three sites in the posterobasal left ventricle during S₁-S₂ stimulation is shown. ARIs and diastolic intervals (in parentheses) from unipolar virtual electrograms—virtuals 6, 8, 10—are determined using their respective first derivatives (dV/dt)—virtuals 7, 9, 11 at the same sites. Maximum ARI restitution slopes from a right ventricular site (B) and left ventricular site (C) are measured by 16 overlapping least-squares linear segments. LVOT = left ventricular outflow tract; MV = mitral valve.

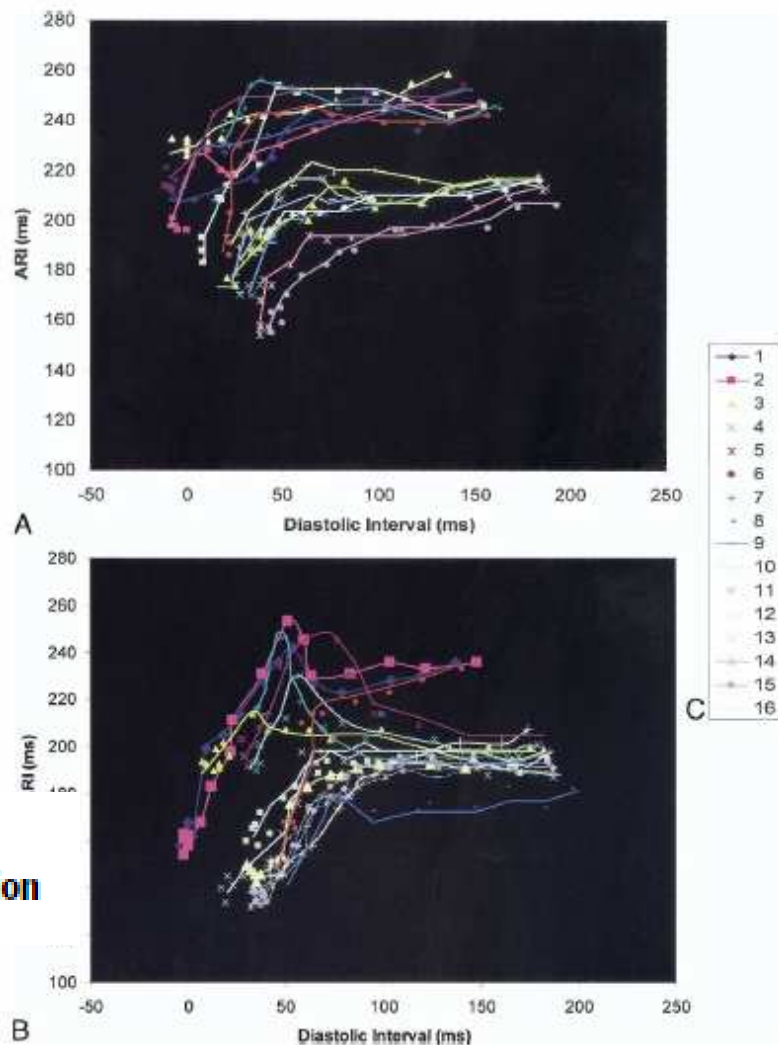


Figure 3. Global activation-recovery interval (ARI) restitution curves. Simultaneous restitution curves were constructed at 16 sites in a right ventricle (A) left ventricle (B). Color labels for the 16 regional segments are illustrated in (C). Locations of the 16 segments are shown in Figure 1.

Alternans and spiral breakup in a human ventricular tissue model

K. H. W. J. ten Tusscher and A. V. Panfilov

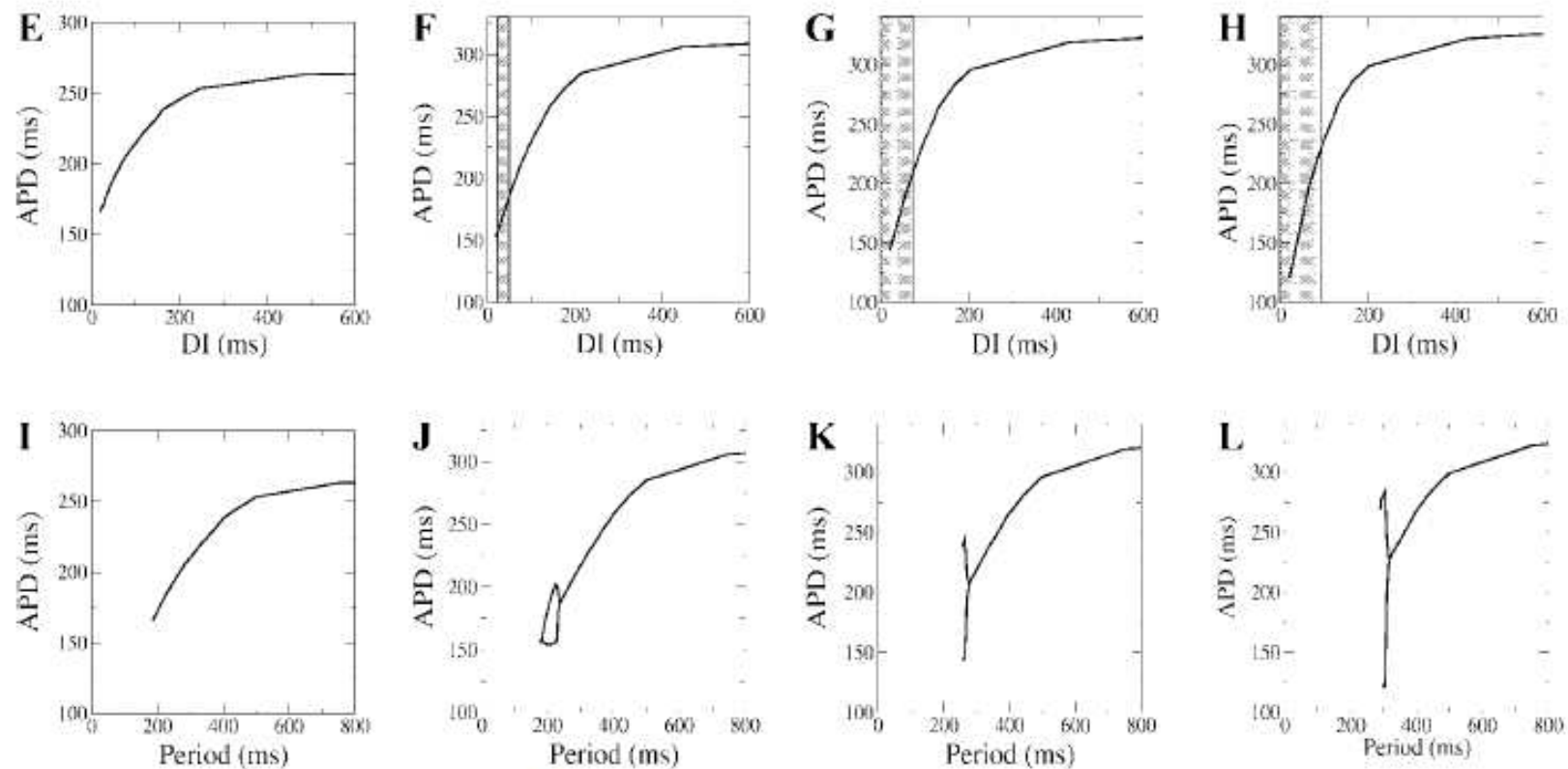


Fig. 5. Single-cell action potential duration (APD) restitution. *A–D*: restitution curves obtained using a S1-S2 restitution protocol for a basic cycle length (BCL) of 600 ms measuring APD at 50% (APD_{50}) and 90% repolarization (APD_{90}) for 4 different parameter settings of our model (Table 2). APD is plotted against diastolic interval (DI). Experimental activation recovery interval (ARI) restitution curves (exp) are from Nash et al. (38–40). *E–H*: restitution curves obtained using a dynamic restitution protocol measuring APD_{90} for the 4 same parameter settings. APD is plotted against DI. Gray shading is used to indicate the region of the restitution curve where the slope exceeds 1. *I–L*: same dynamic restitution curves as in *E–H*, but now plotting APD against stimulation period. Splitting of the restitution curve indicates the presence of 2 APDs for a single period: APD alternans.

Atrial Fibre & Ventricular Fibre Action Potentials

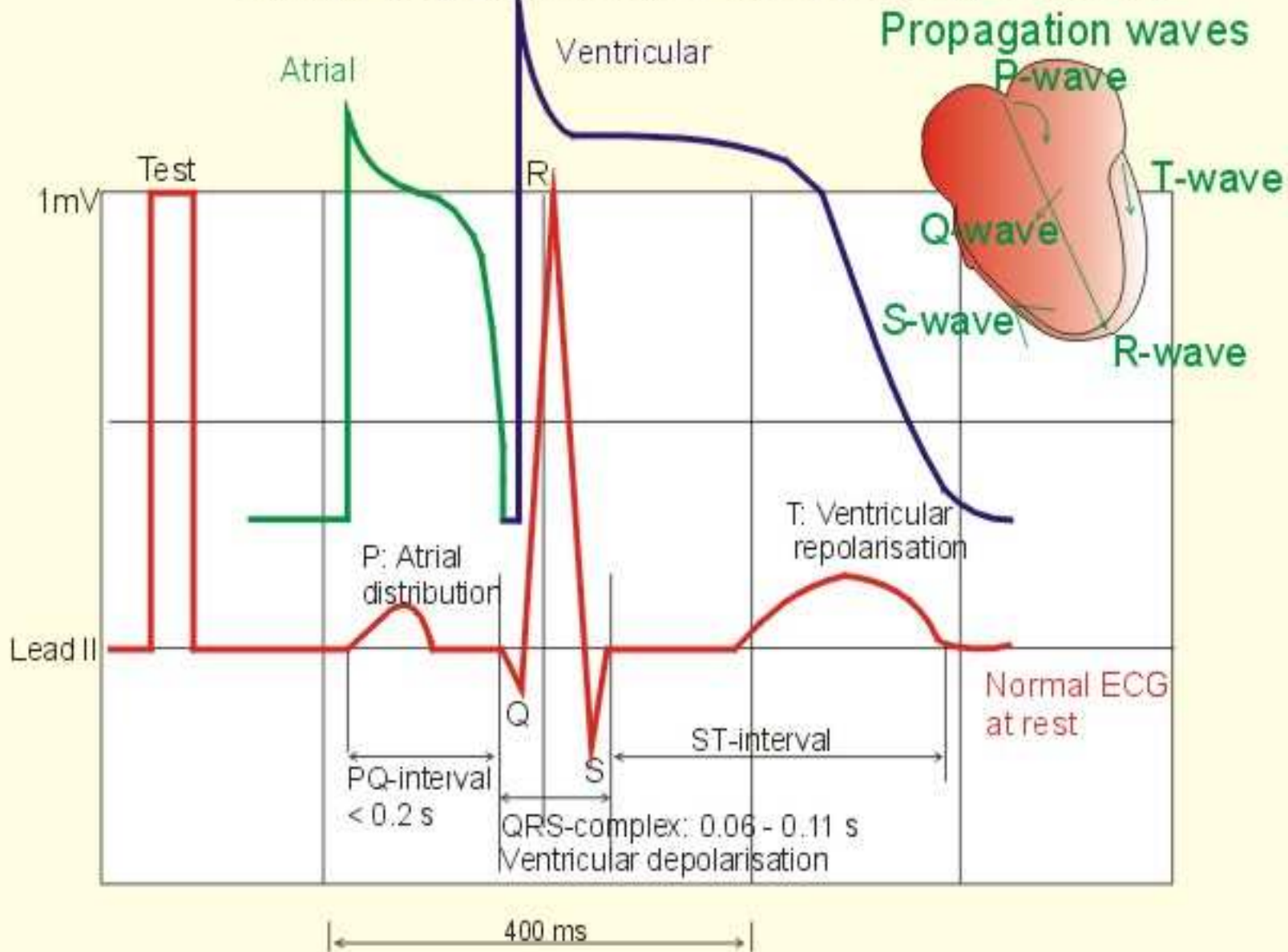
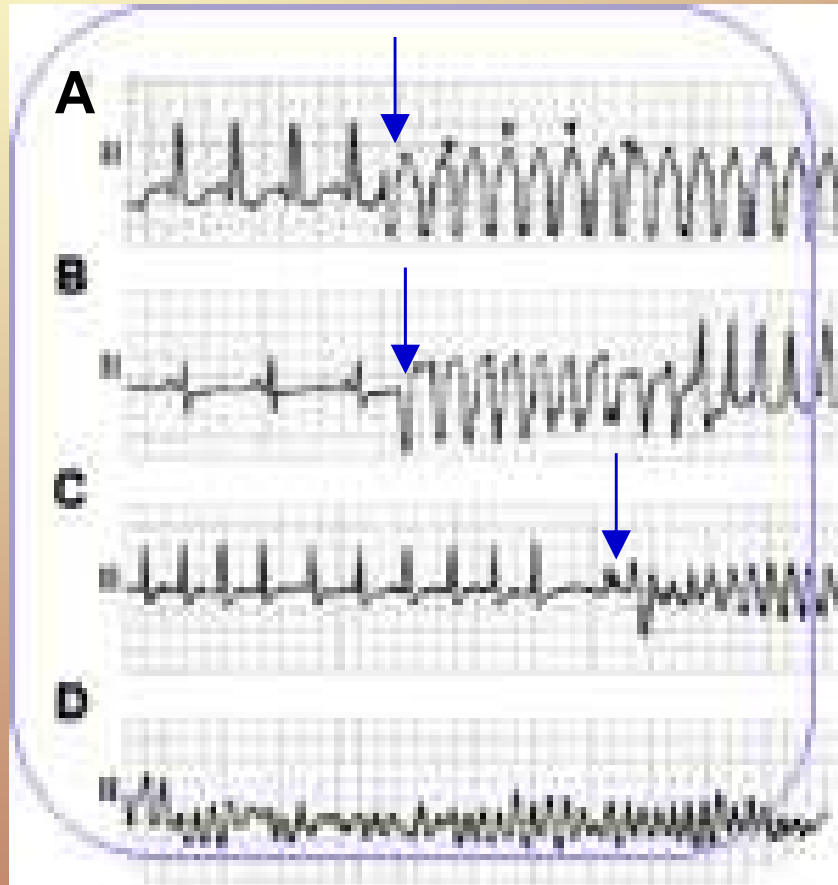


Fig. 11-6

KMc

Poul-Erik Paulev Medical Physiology and Pathophysiology. Essentials and clinical problems. Copenhagen Medical Publishers. 1999 – 2000, <http://www.mfi.ku.dk/PPaulev/chapter11/Chapter%2011.htm>

Why life threatening arrhythmias always suddenly start and stop?



Roughly half of the deaths caused by cardiovascular disease are sudden. The majority of those sudden deaths – an estimated 300 000 per year in US – are associated with ventricular fibrillation.

Factors known to trigger or modulate VT/VF

**Goldberger J. J. et al. Risk Stratification for Sudden Death
JACC, V. 52, N. 14, 1179 –99. 2008**

- changes in autonomic nervous system activity,
- metabolic disturbances,
- myocardial ischemia,
- electrolyte abnormalities,
- acute volume and/or pressure overload of the ventricles,
- ion channel abnormalities,
- proarrhythmic actions of cardiac and noncardiac drugs.

**Michael Rubart and Douglas P. Zipes, Mechanisms of
sudden cardiac death, *J. Clin. Invest.* 115,2305 (2005).**

*“ However, these factors alone cannot explain the
apparent **randomness** of the occurrence of fatal
arrhythmias ”*

Multistability

- the coexistence of several stable states of a system at a fixed set of stimulation parameters;
- each of the stable states realizes from different initial conditions.

Bistability observations in vivo (animal) experiments



- Mines G. R. On dynamic equilibrium in the heart. *Journal of Physiology (London)* V. 46, P. 349–383, 1913. (in frog)
- Nolasco J. B. and Dahlen R. W., A graphic method for the study of alternation in cardiac action potentials. *Journal of Applied Physiology* 25, 191–196, 1968. (in frog)
- Yehia A. R., Jeandupeux D., Alonso F., Guevara M. R., Hysteresis and Bistability in the Direct Transition from 1:1 to 2:2 Rhythm in Periodically Driven Single Ventricular Cells. *Chaos*. V. 9(4), P. 916–931, 1999. (in rabbit)
- Hall G. M., Bahar S, Gauthier D. J. Prevalence of rate-dependent behaviors in cardiac muscle. *Phys. Rev. Lett.* V. 82, P. 2995–2998, 1999. (in bullfrog)
- Bien H. Cardiac arrhythmogenesis in urban air pollution: optical mapping in a tissue-engineered model, Doctoral thesis, Stony Brook University, 2007. (in rat)

Hodgkin-Huxley Ionic Current Model

Hodgkin, A.L. and A.F. Huxley, A quantitative description of membrane current and its application to conduction and excitation in nerve. J Physiol, 1952. 117: p. 500-544.

Ohm's Law:

$$I_K = g_K (V_m - E_K)$$

$$I_{Na} = g_{Na} (V_m - E_{Na})$$

$$I_{Cl} = g_{Cl} (V_m - E_{Cl})$$

Nernst potentials:

$$E_K = \frac{RT}{F} \ln \left(\frac{[K]_o}{[K]_i} \right)$$

$$E_{Na} = \frac{RT}{F} \ln \left(\frac{[Na]_o}{[Na]_i} \right)$$

$$E_{Cl} = \frac{RT}{F} \ln \left(\frac{[Cl]_o}{[Cl]_i} \right)$$

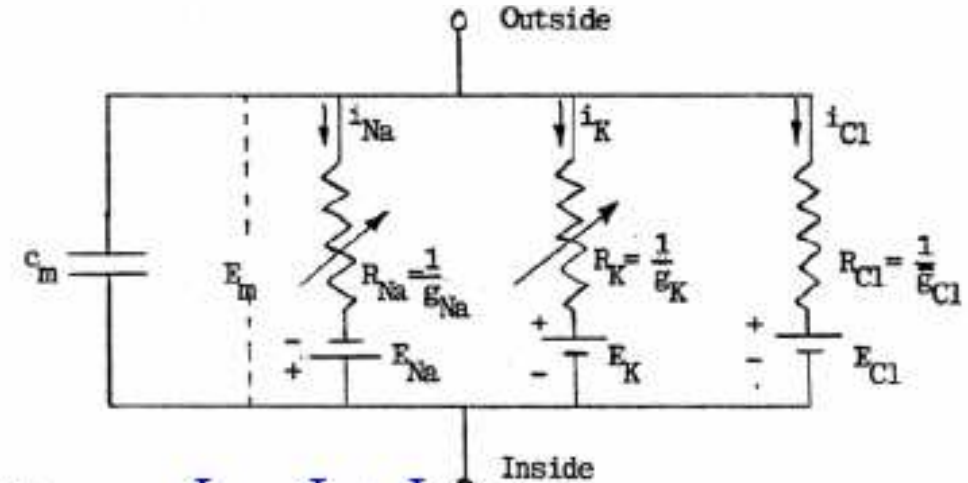
Conductances (1/resistance):

$$g_K = \bar{g}_K n^4$$

$$g_{Na} = \bar{g}_{Na} m^3 h$$

$$g_{Cl} = \bar{g}_{Cl}$$

Gating variables: n , m , and h



Kirchhoff's current law:

$$I_m = I_c + I_{ion}$$

$$= C_m \frac{dV_m}{dt} + I_{Na} + I_K + I_{Cl}$$

4 ODEs:
For 3 gating variables and membrane potential:

$$\frac{dn}{dt} = \alpha_n (1-n) - \beta_n n$$

$$\frac{dm}{dt} = \alpha_m (1-m) - \beta_m m$$

$$\frac{dh}{dt} = \alpha_h (1-h) - \beta_h h$$

α is rate of channel opening; β is rate of channel closing; α and β are functions of determined by experimental curve fit

$$-C_m \frac{dV_m}{dt} = \bar{g}_K n^4 (V_m - E_K) + \bar{g}_{Na} m^3 h (V_m - E_{Na}) + \bar{g}_{Cl} (V_m - E_{Cl})$$

A single cell model

The rate of change of transmembrane potential is given by

$$dV / dt = (-I_{ion} + I_{stim}) / C$$

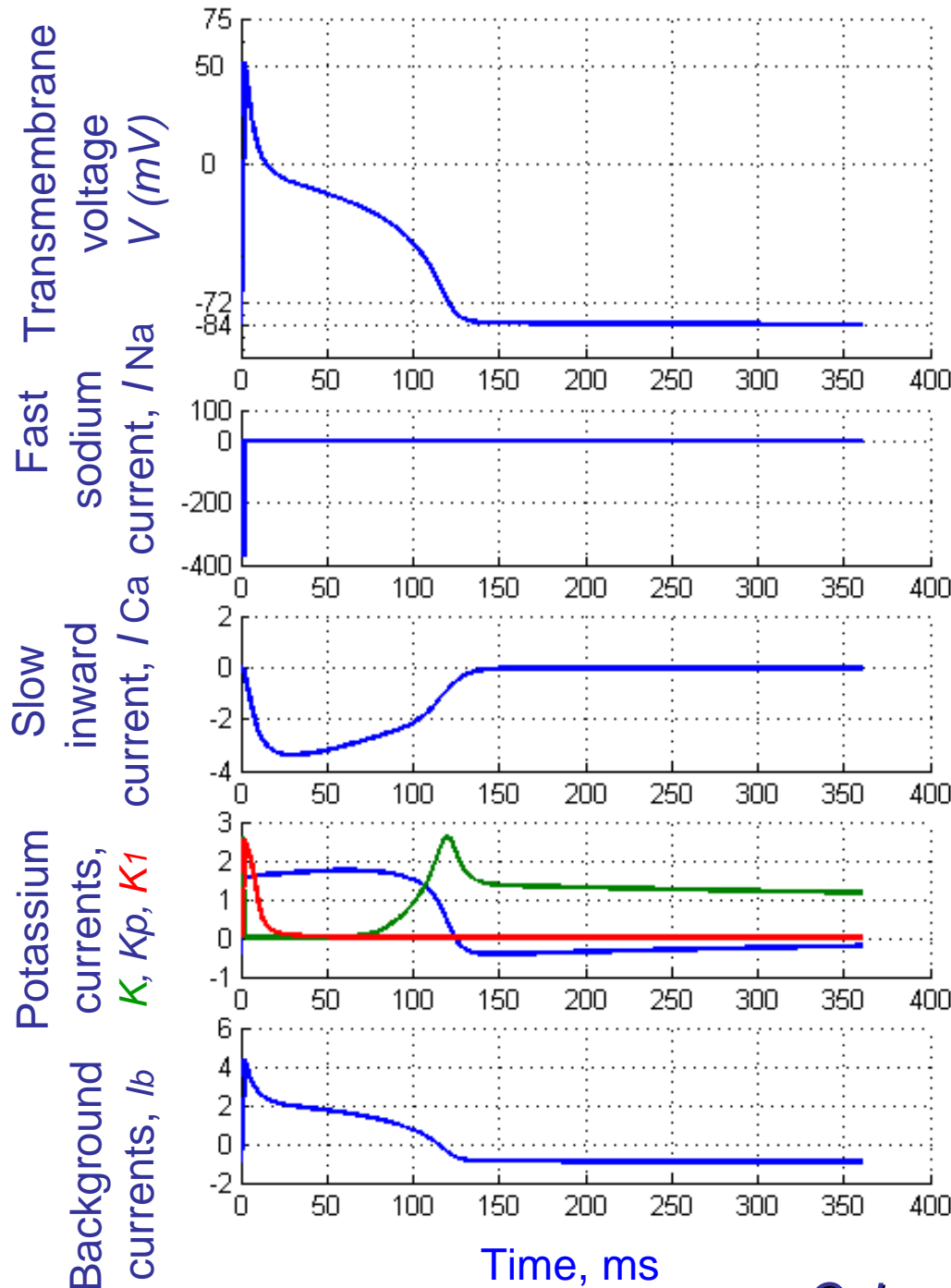
- I_{ion} - the total transmembrane ionic current, determined by choice of cellular ionic model
- I_{stim} - a stimulus current,
- C - the membrane capacitance

Ionic models are increasingly detailed:

- ✓ Noble¹ – 4 ODEs
- ✓ Luo-Rudy² – 8 ODEs
- ✓ Ten Tusscher - Panfilov³ – 19 ODEs
- ✓ Flaim-Giles-McCulloch⁴ – 87 ODEs

¹Noble 1962; ²Luo *et al.* 1991; ³Ten Tusscher & Panfilov 2006; ⁴Flaim *et al.* 2006

Luo-Rudy model ...



$$\leftarrow \frac{dV}{dt} = \frac{(-I_{ion} + I_{stim})}{C_m}$$

$$I_{ion} = I_{Na} + I_{Ca} + I_K + I_{K_1} + I_{Kp} + I_b$$

Ionic currents

$$\leftarrow I_{Na} = 23m^3hj(V - E_{Na})$$

$$\leftarrow I_{Ca} = G_{Ca} \cdot d \cdot f \cdot (V - E_{Ca}),$$

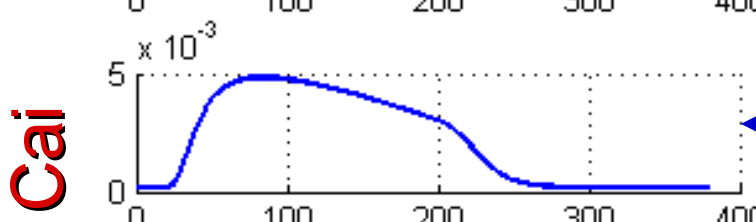
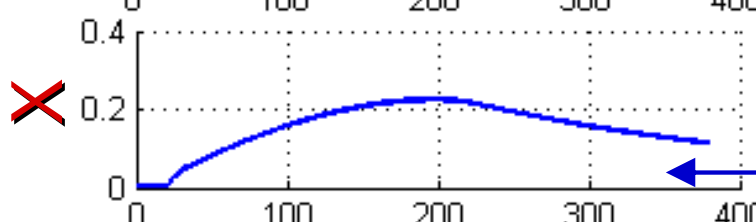
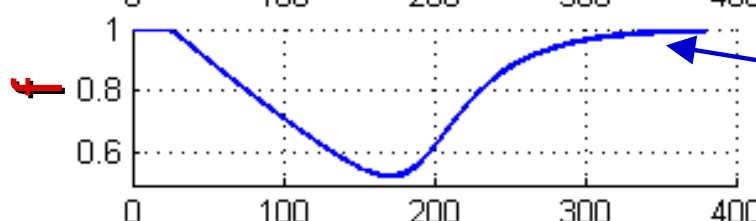
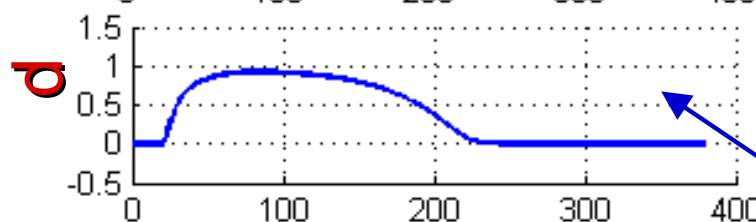
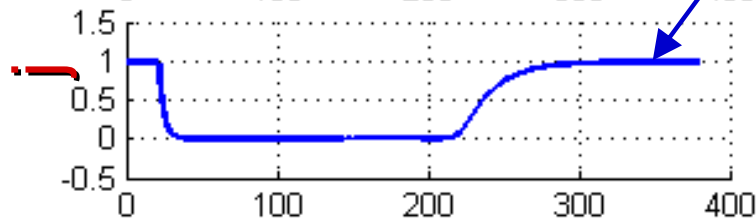
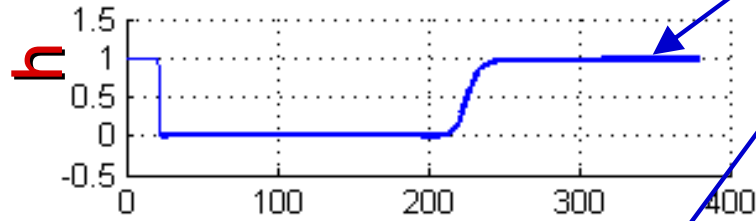
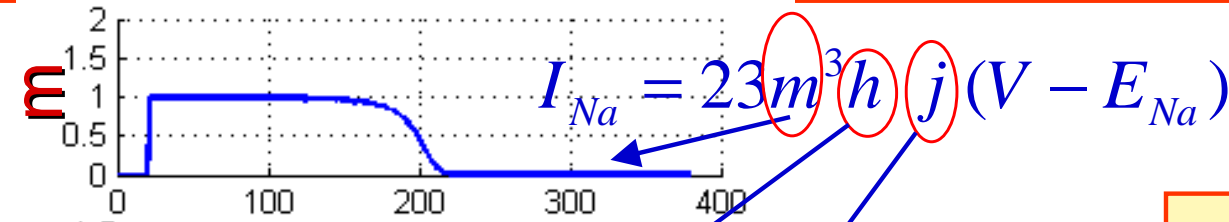
$$\leftarrow I_k = \bar{G}_k \cdot X \cdot X_i \cdot (V - E_k),$$

$$\leftarrow I_{k1} = \bar{G}_{k1} \cdot K1_{\infty} \cdot (V - E_{k1}),$$

$$\leftarrow I_{Kp} = 0.0183 \cdot K_p \cdot (V - E_{Kp}),$$

$$\leftarrow I_b = 0.03921 \cdot (V + 59.87)$$

Ionic gates



$$\frac{dy}{dt} = \frac{(y_{\infty} - y)}{\tau_y}$$

$$\tau_y = \frac{1}{\alpha_y + \beta_y} \quad y_{\infty} = \frac{\tau_y a_y}{\alpha_y + \beta_y}$$

$$\alpha_y = f(V), \quad \beta_y = f(V)$$

α_y - rate of channel opening
 β_y - rate of channel closing

$I_{Ca} = G_{Ca} \cdot d \cdot f \cdot (V - E_{Ca}),$

$I_k = \bar{G}_k \cdot X \cdot X_i \cdot (V - E_k),$

$d([Ca]_i) / dt = -10^{-4} \cdot I_{Ca} + 0.07(10^{-4} - [Ca]_i)$

Time, ms

$$dy/dt = (y_\infty - y) / \tau_y \quad y_\infty = \frac{a_y}{\alpha + \beta} \quad \tau_y = \frac{1}{\alpha + \beta}$$

$$I_{Na} = 23 m^3 h j (V - E_{Na})$$

For all range of V

$$\alpha_m = \frac{0.32(V + 47.13)}{1 - \exp[-0.1(V + 47.13)]}$$

$$\beta_m = 0.08 \exp\left(-\frac{V}{11}\right)$$

For $V > -40 \text{ mV}$

$$\alpha_h = a_j = 0$$

$$\beta_j = \frac{0.3 \exp(-2.535 \cdot 10^{-7} V)}{1 + \exp[-0.1(V + 32)]}$$

$$\beta_h = \frac{1}{0.13(1 + \exp[V + 10.66] / -11.1)}$$

For $V < -40 \text{ mV}$

$$\alpha_h = 0.135 \exp[(80 + V) / -6.8]$$

$$\beta_h = 3.56 \exp(0.079 V) + 3.1105 \exp(0.35 V)$$

$$\alpha_j = \frac{[-1.2714 \cdot 10^5 \cdot \exp(0.2444 V) - 3.474 \cdot 10^5 \cdot \exp(-0.04391 V)](V + 37.78)}{1 + \exp[0.311(V + 79.23)]}$$

$$\beta_j = \frac{0.1212 \cdot \exp(-0.01052 V)}{1 + \exp(-0.1378(V + 40.14))}$$

$$I_{Ca} = G_{Ca} \cdot d \cdot f \cdot (V - E_{Ca}),$$

$$E_{Ca} = 7.7 - 13.0287 \cdot \ln([Ca]_i)$$

$$\alpha_d = \frac{0.095 \cdot \exp[-0.01(V - 5)]}{1 + \exp[-0.072(V - 5)]}$$

$$\beta_d = \frac{0.07 \cdot \exp[-0.017(V + 44)]}{1 + \exp[0.05(V + 44)]}$$

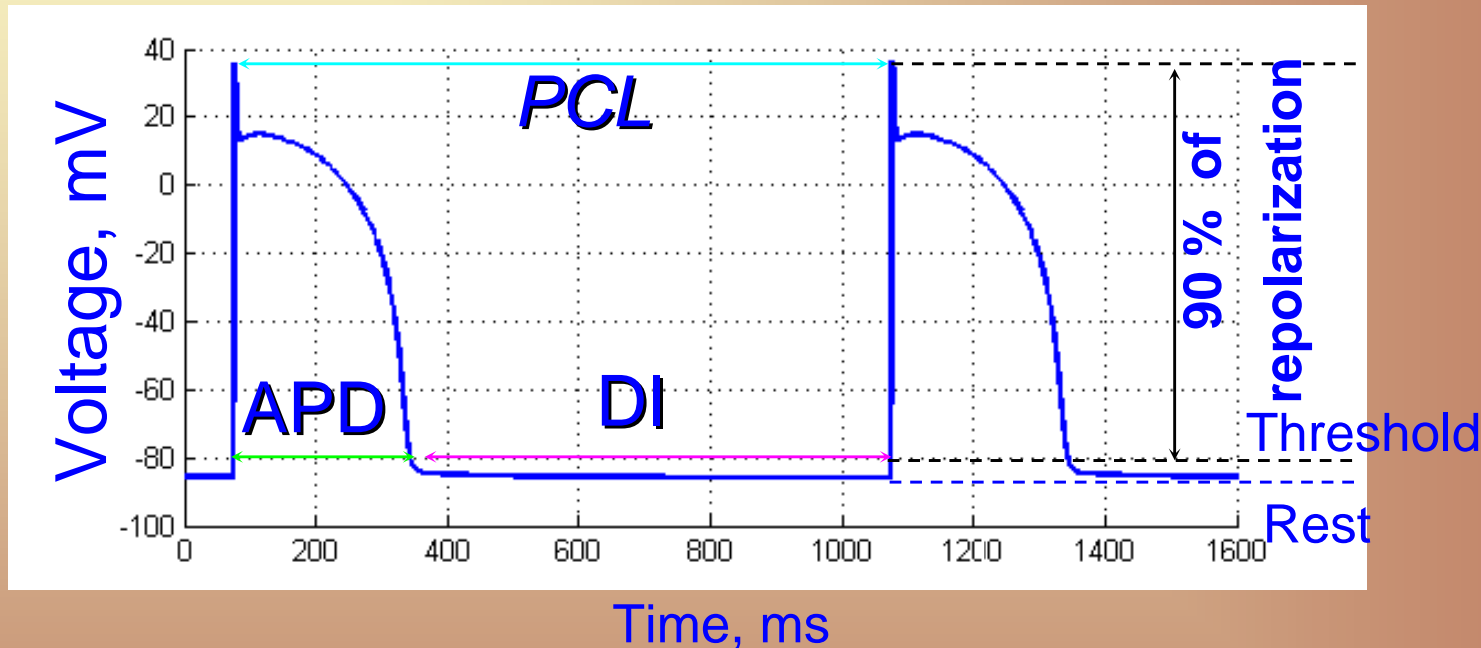
$$\alpha_f = \frac{0.012 \cdot \exp[-0.008(V + 28)]}{1 + \exp[0.15(V + 28)]}$$

$$\beta_f = \frac{0.0065 \cdot \exp[-0.02(V + 30)]}{1 + \exp[-0.2(V + 30)]}$$

$$d([Ca]_i) / dt = -10^{-4} \cdot I_{Ca} + 0.07(10^{-4} - [Ca]_i)$$

ACTION POTENTIAL

$$dV/dt = (-I_{ion} + I_{stim}) / C$$

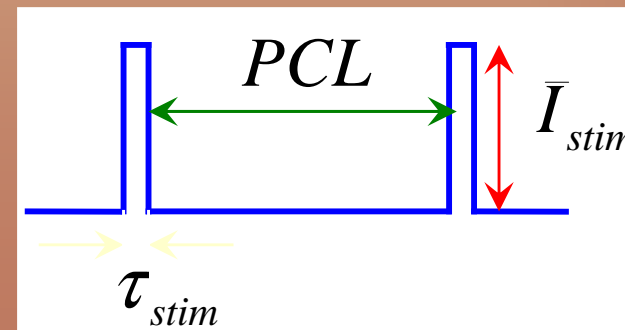


APD - action potential duration

DI - diastolic interval

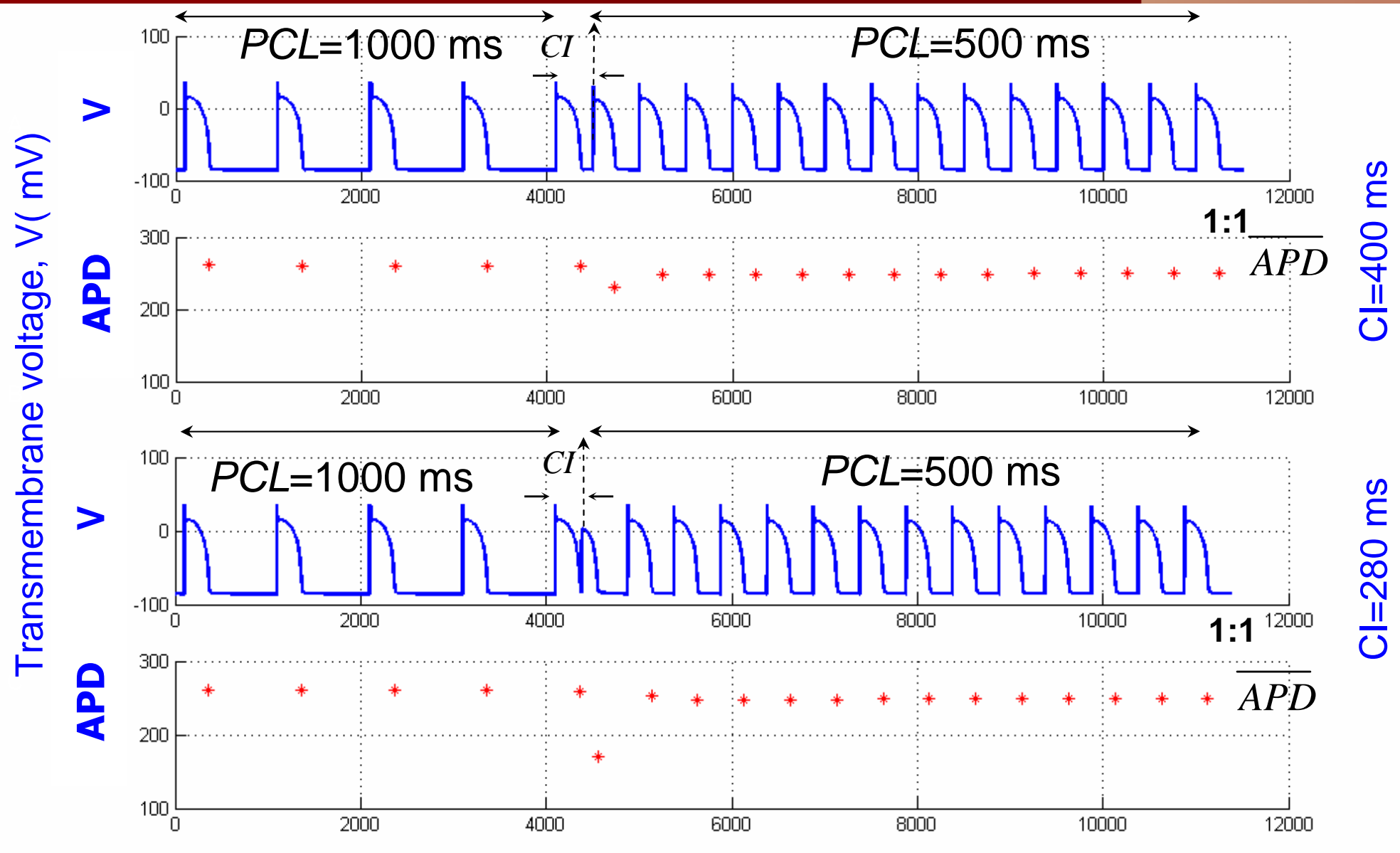
PCL - pacing cycle length

I_{stim} - stimulus current

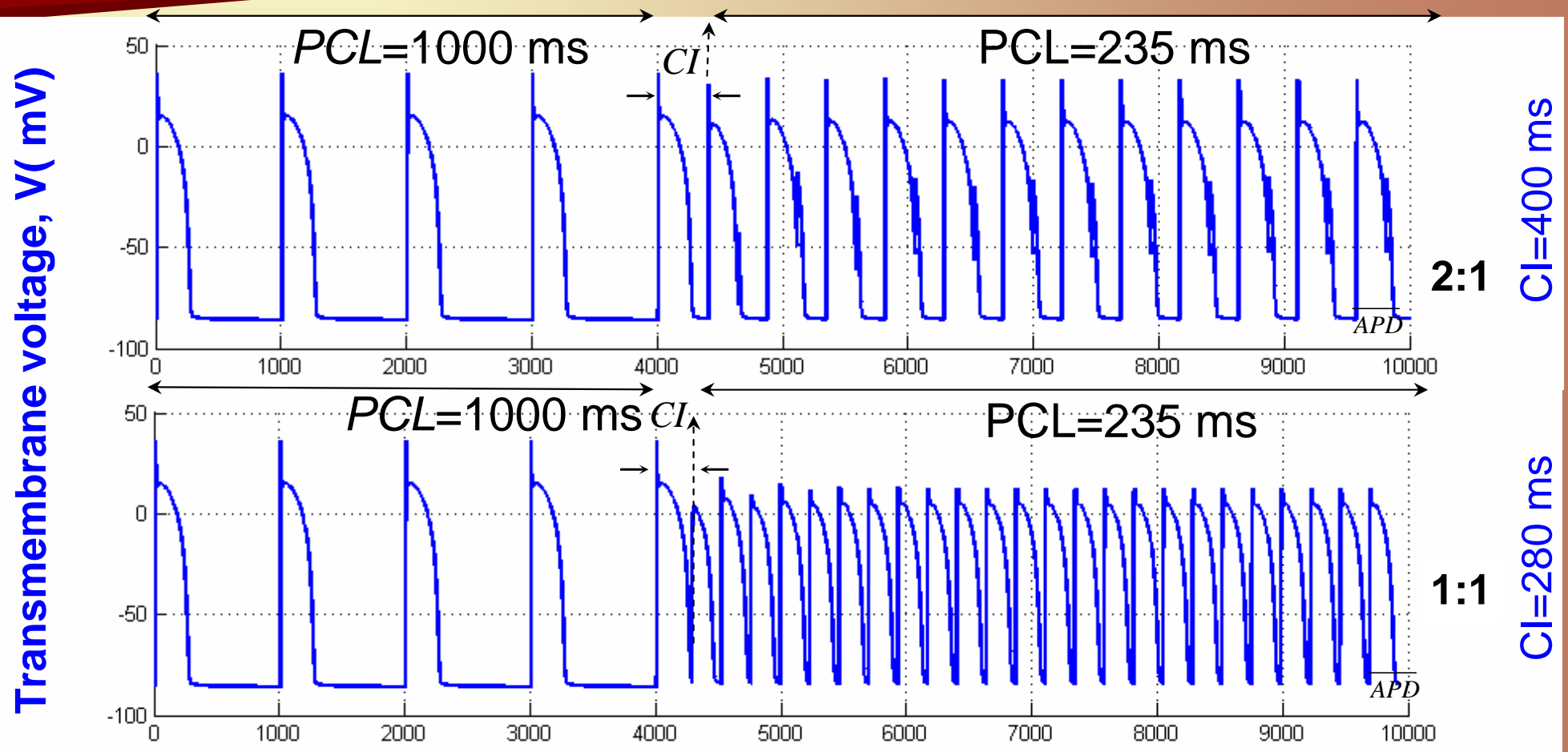


The S1-CI-S2 protocol of stimulation

(Surovyatkina et al. 2007, 2010)

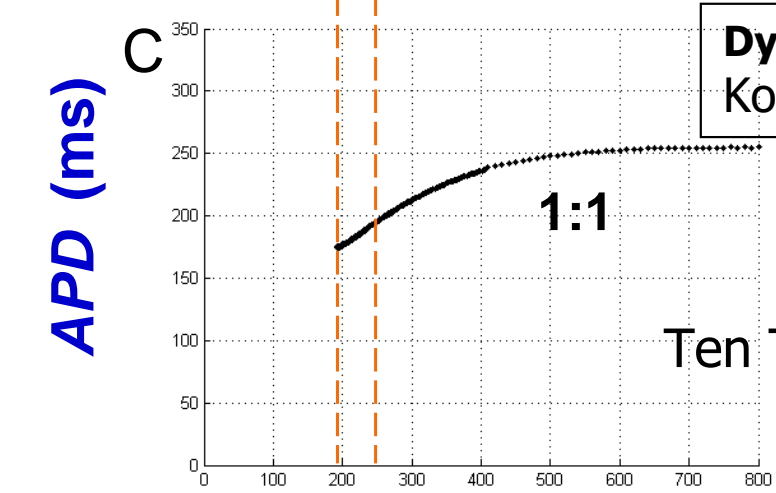
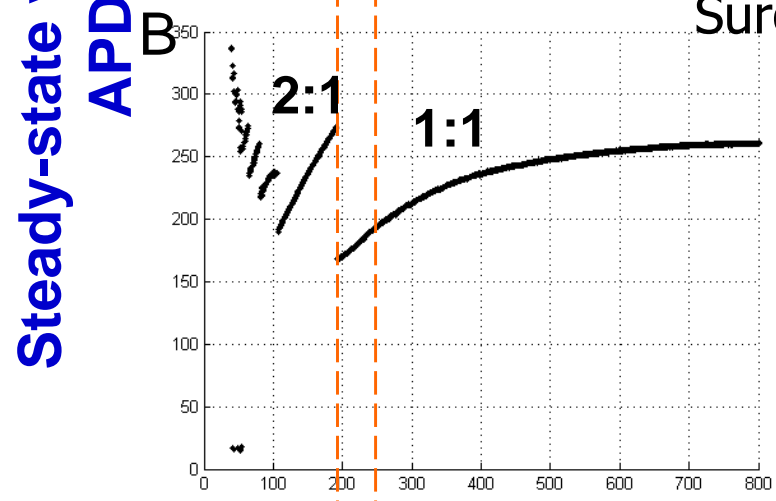
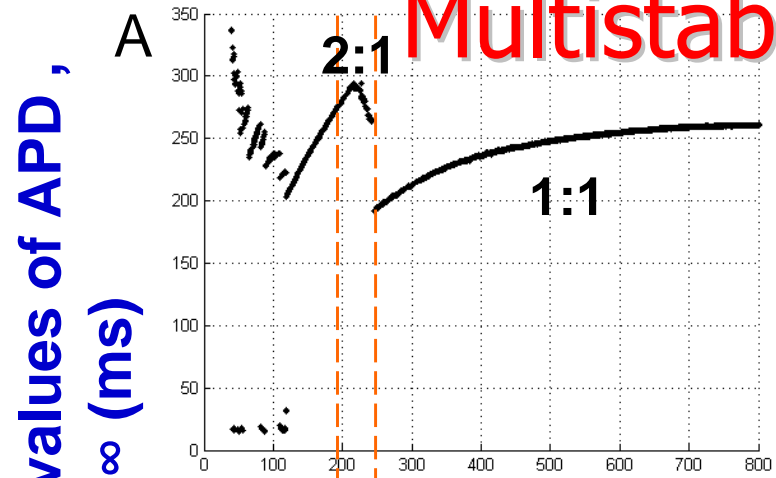


Multistability in the human ventricular single cell model



Coexistence of 2:1- & 1:1- rhythms 20

Multistability in human myocyte

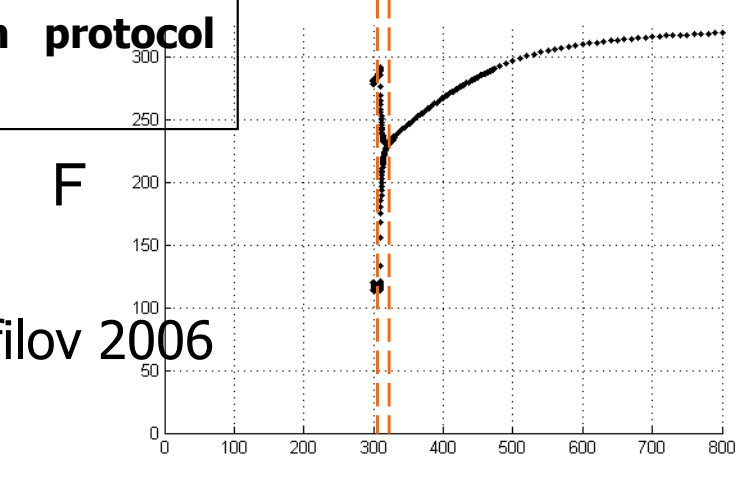
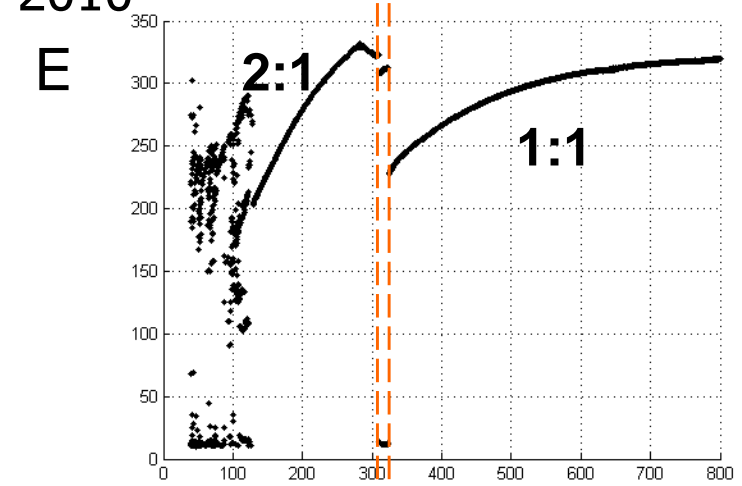
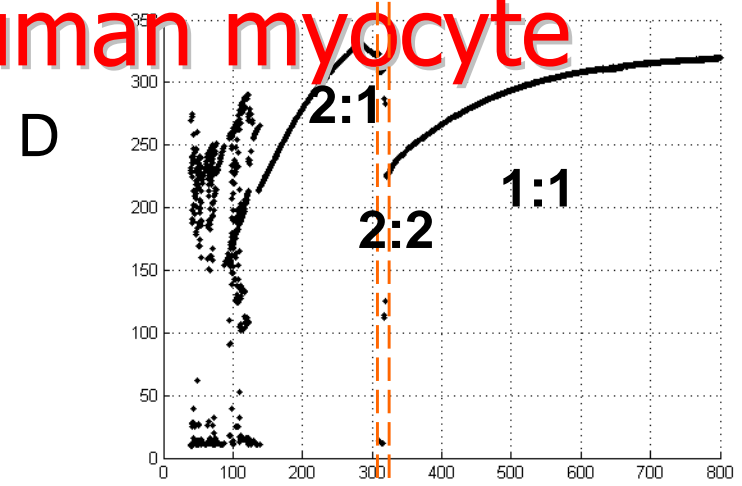


Surovyatkina et al. 2010

Dynamic restitution protocol
Koeller et al. 1998

Ten Tusscher & Panfilov 2006

Pacing cycle length (PCL), ms



CI=400 ms

CI=280 ms

Conclusion

Why life threatening arrhythmias suddenly start and stop?

1. The additional mechanism of sudden change in heart rhythm based on the multistability property of the human ventricular cells is proposed.
2. The multistability mechanism may explain the apparent randomness of the occurrence of fatal arrhythmias in the human heart.

Multistability in Models of Mammalian and Human Cardiac Ventricular Cells

- Surovyatkina E., Egorchenkov R., Ivanov G. **Multistability as intrinsic property of a single cardiac cell: a simulation study**//Conf Proc IEEE Eng Med Biol Soc.1-4244-0788-5/07. 2007. P. 927-930.
- Surovyatkina E., Noble D., Gavaghan D., Sher A. Multistability Phenomenon in Ionic Models of Mammalian and **Human Cardiac Ventricular Cells**. Progress in Biophysics and Molecular Biology. [doi:10.1016/j.pbiomolbio.2010.01.004](https://doi.org/10.1016/j.pbiomolbio.2010.01.004) , 2010.



Listen to your heart....

Thank you!